ALTMANN, S. L. (1963*b*). *Rev. Mod. Phys.* **35**, 641-645.
BRADLEY, C. J. & CRACKNELL, A. P. (1972). *The Mathematical Theory of Symmetry in Solids.* Oxford: Clarendon Press.
VEYSSEYRE, R., PHAN, T. & WEIGEL, D. (1985). *C.R. Acad. Sci.* **300**, 51-54.
VEYSSEYRE, R., WEIGEL, D., PHAN, T. & EFFANTIN, J. M. (1984). *Acta Cryst.* A**40**, 331-337.
WEIGEL, D., PHAN, T. & VEYSSEYRE, R. (1984). *C.R. Acad. Sci.* **298**, 825-828.
WEIGEL, D. & VEYSSEYRE, R. (1982). *C.R. Acad. Sci.* **295**, 317-322.
WEIGEL, D., VEYSSEYRE, R., PHAN, T., EFFANTIN, J. M. & BILLIET, Y. (1984). *Acta Cryst.* A**40**, 323-330.
WHITTAKER, E. J. W. (1984). *Acta Cryst.* A**40**, 404-410.
WOLFF, P. M. DE, JANSSEN, T. & JANNER, A. (1981). *Acta Cryst.* A**37**, 625-636.
WONDRATSCHEK, H., BÜLOW, R. & NEUBÜSER, J. (1971). *Acta Cryst.* A**27**, 523-535.

Acta Cryst. (1987). A**43**, 304-316

Extinction in the Framework of Transfer Equations for General-Type Crystals

BY N. C. POPA*

Laboratory of Neutron Physics, Joint Institute for Nuclear Research, Dubna, Head Post Office, PO Box 79, Moscow, USSR

(*Received* 31 *October* 1985; *accepted* 20 *October* 1986)

Abstract

An improvement of the classical theory of extinction in mosaic crystals is made by starting from the energy transfer equations valid for a general-type crystal according to Zachariasen's [*Acta Cryst.* (1967), **23**, 558-564] classification. Within the assumption that only the integrated intensity of the diffraction peak is needed, the equations are first simplified and then solved. The result obtained for the extinction factor is similar to that of Becker & Coppens [*Acta Cryst.* (1974), A**30**, 129-147], but two new parameters appear if the crystal is not of type I. One of them, determining the peculiarity of the transfer equations, gives differences in the extinction factor not greater than 8%. The other, representing the ratio of the kinematical cross-section strengths along the diffracted and incident beams, gives differences up to 50%. For crystals of ellipsoidal shape, empirical formulae appropriate for structure refinement programs are proposed.

1. Introduction

In this paper we re-analyse the problem of secondary extinction in the framework of classical transfer theory. The transfer equations for secondary extinction in finite crystals were first written by Hamilton (1957) and were based on the mosaic model of Darwin (1922) for the ideal imperfect crystal. Zachariasen (1967) has used similar equations to describe extinction in real crystals, so henceforth we will call these equations Hamilton-Zachariasen (HZ) equations. Zachariasen stated that any real crystal is situated between two limiting types, distinguished by the nature of the peak width: type I if the width is given exclusively by the mosaic and type II if the width is given by the crystallite size only. Correspondingly, the secondary extinction follows the same classification. So far as primary extinction in small mosaic blocks is concerned, a description by the same transfer equations has been considered good enough under the assumption that this extinction is weak. The unified theory of Zachariasen has been very much criticized both for some mathematical errors and for its physical basis. On the same basis, Becker & Coppens (1974*a*) (BC) have re-analysed the HZ equations. The solution which they provided has become very popular both for its convenient parametrization for least-squares-refinement programs and for its resistance to numerous experimental tests (see *e.g.* Hutton, Nelmes & Scheel, 1981).

The limitations on the classical theory of extinction in real crystals were clarified by the new dynamical statistical theory of Kato (1976*a*, *b*, 1979, 1980). Starting from the dynamical equations for a distorted crystal and assuming a homogeneous and isotropic distribution of the defects, Kato derived a system of energy transfer equations valid for extinction only if the coherence distance t_c is smaller than the extinction distance $\Lambda = (n\lambda|F|)^{-1}$. Here λ is the wavelength, F the structure factor and n the density of unit cells. The energy transfer equations of Kato are similar to but not identical with the HZ equations. The differences discussed in detail by Kato (1976*b*, 1979) are in the form and physical interpretation of the coupling constants. Analysing the equivalence between the two kinds of energy transfer equations, Becker (1977) concludes that the range of validity found by Kato

* Permanent address: Institute for Nuclear Power Reactors, PO Box 78, Pitesti, Romania.

0108-7673/87/030304-13$01.50

for his energy transfer equations is the same for the HZ equations. The Kato theory, giving the extinction for any degree of crystal perfection, is more extensive than the classical theory. For $t_c > \Lambda$ the Kato theory replaces the energy transfer equations by equations for the averaged wave functions. On the basis of Kato's energy transfer equations, Kawamura & Kato (KK) (1983) have elaborated a practical formula for the secondary extinction in a cylinder and a sphere, valid for a Bragg angle smaller than 30° and extinction parameter smaller than 2. Comparing their formula numerically with the BC calculations, KK have found significant differences. But recently Harada, Miyatake & Sakata (1984) have compared KK and BC formulae experimentally using neutron diffraction data. Although some reflections were severely affected by extinction, they have found only small differences in the refined structure parameters.

It seems that in spite of its limitations there are not enough arguments for abandoning the classical theory of secondary extinction. But as was emphasized for a long time (Werner, 1974) the HZ equations describe the secondary extinction rigorously only in crystals of type I. When the natural broadening becomes competitive with the mosaic broadening or dominant, the classical energy transfer equations take a different form, the HZ equations being only a limiting case. These more general equations, labelled below as (1), can be directly obtained (see *e.g.* Popa, 1976) from the neutron transport equation of Vineyard (1954), which is a classical equation (see *e.g.* Sears, 1975, 1978). Thus the equations (1) are also classical, and like their HZ limits they describe the extinction only for crystals and diffraction maxima which fulfil the condition given above: $t_c \lesssim \Lambda$. This condition is fulfilled by type II rather than by type I crystals. Indeed the type II extinction is associated with a small block size, while in type I crystals the block size and the primary extinction may be large. In this paper we solve (1) in order to find a formula for the secondary extinction (alternative to BC) valid (in the limit $t_c \lesssim \Lambda$) for any type of crystals: type I, type II and a mixed type. The correction to the BC result is small for isotropic crystals of type II, but becomes significant for anisotropic crystals. This may explain why in many cases the BC formula fits the experimental data well, but sometimes, although the mosaic is small, the type II model for extinction gives an odd result (see Hutton, Nelmes & Scheel, 1981).

This paper contains six parts. In § 2 the arguments permitting simplification of the transfer equations which are then solved in the next two parts are discussed. Two new quantities are defined, which differentiate our result from the BC result. In § 5 an empirical formula is proposed for extinction in spherical and ellipsoidal crystals with anisotropy. A comparison with the BC result is made in § 6.

2. Transfer equations for intensities

For small primary extinction and weak absorption the general form of the energy transfer equations is (Werner, 1974)

$$\partial I_1(\mathbf{r}, \mathbf{k}_1)/\partial x_1 = -[\mu + \textstyle\int \mathrm{d}\mathbf{k}_2\, \bar{\sigma}(\mathbf{k}_1 \to \mathbf{k}_2)] I_1(\mathbf{r}, \mathbf{k}_1) + \textstyle\int \mathrm{d}\mathbf{k}_2\, \bar{\sigma}(\mathbf{k}_2 \to \mathbf{k}_1) I_2(\mathbf{r}, \mathbf{k}_2). \quad (1a)$$

$$\partial I_2(\mathbf{r}, \mathbf{k}_2)/\partial x_2 = -[\mu + \textstyle\int \mathrm{d}\mathbf{k}_1\, \bar{\sigma}(\mathbf{k}_2 \to \mathbf{k}_1)] I_2(\mathbf{r}, \mathbf{k}_2) + \textstyle\int \mathrm{d}\mathbf{k}_1\, \bar{\sigma}(\mathbf{k}_1 \to \mathbf{k}_2) I_1(\mathbf{r}, \mathbf{k}_1). \quad (1b)$$

The indices 1 and 2 refer to the incident and diffracted beams respectively, I is the intensity, $\mathbf{k}$ is the wave vector, μ is the linear absorption coefficient (including all non-Bragg scattering). x_1, x_2 are the coordinates in the oblique system with axes $\mathbf{i}_1$, $\mathbf{i}_2$ along the mean incident and diffracted beam respectively and $\mathbf{i}_3$ normal to the $(\mathbf{i}_1, \mathbf{i}_2)$ plane, which in the following will be considered horizontal (see Fig. 1). The quantity $\bar{\sigma}(\mathbf{k}_1 \to \mathbf{k}_2)$ is the average over the mosaic distribution of the kinematical Bragg cross section per unit volume for the process $\mathbf{k}_1 \to \mathbf{k}_2$. It is independent of $\mathbf{r}$ if the crystal is homogeneous. If the primary extinction factor y_p is not unity and the average size of the perfect crystallites is smaller than the extinction distance, then the same equations (1) will be used with replacement of $\bar{\sigma}$ by $y_p\bar{\sigma}$.

The explicit form of the cross section $\bar{\sigma}$ depends on the model chosen for the crystal microstructure: the shape and the dimension of the perfect blocks and the distribution of their orientations. The model frequently used for the anisotropic mosaic crystals has at most twelve parameters. These are the lengths and the orientations of the principal axes of two ellipsoids; one ellipsoid approximates the average shape of the perfect mosaic block (Coppens & Hamilton, 1970) and the second is the surface of constant probability associated with the three-dimensional distribution function $W(\boldsymbol{\Delta})$ describing the block misorientations (Nelmes, 1980). Here $\boldsymbol{\Delta}$ is a vector of which components represent small rotations around

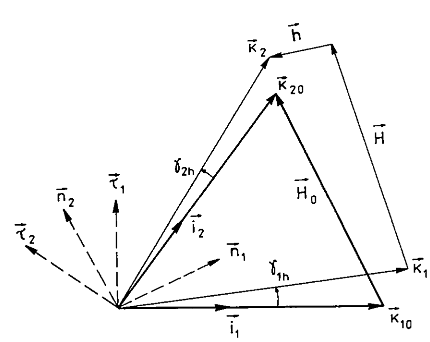

Fig. 1. Diagram of the diffraction process and the coordinate systems (**i**), (**τ**), (**n**). The wave vectors $\mathbf{k}_1$, $\mathbf{k}_2$ are drawn for convenience in the plane of their averages, $\mathbf{k}_{10}$ and $\mathbf{k}_{20}$, respectively. The unit vectors $\mathbf{i}_3 = \boldsymbol{\tau}_3 = \mathbf{n}_3$ are perpendicular to the plane of the figure.

the axes of an orthogonal coordinate system. The number of model parameters reduces to two if no anisotropy exists, and to one if, moreover, the crystal is of type I or type II.

The Bragg cross section is elastic. It contains the factor $\delta(\mathbf{k}_1-\mathbf{k}_2)$ (which in the following will be omitted); thus all the integrals in (1) become double integrals.

If the profile of the diffraction peak is desired, (1) must be solved under the boundary conditions imposed by the instrument. But both the boundary conditions and (1) become simpler if one wants only the integrated intensity of the diffraction peak, a quantity independent of resolution. There are many possible ways to record the integrated intensity. If, for example, the diffractometer is set to have a very good resolution, a three-dimensional scan must be performed. The dimension of the scan can be decreased if the resolution is reduced. For example, if the collimator in front of the detector is removed and the detector's window is large enough, the integrated intensity is provided by a one-dimensional scan. For the angular dispersive diffraction method this may be a scan with the crystal (detector fixed) or a scan with the crystal and detector in the ratio 1:2. If a strongly divergent monochromatic beam with uniform angular distribution of intensity is available, the integrated intensity can be measured with both crystal and detector fixed (no scan). For the integrated intensity all these procedures are equivalent, the practical choice being dictated by other considerations. The last procedure entailing the simplest boundary conditions for (1) is the most convenient for our aim. In the energy dispersive method the integrated intensity measurement without scan may be realized if the channel width of the energy analyser is chosen large enough to cover the entire diffraction peak. In this method the incident beam is well collimated, but it has uniform wavelength distribution of intensity. In the following the angular dispersive method and the energy dispersive method will be treated together, as they are characterized by the same extinction factor (Tomiyoshi, Yamada & Watanabe, 1980).

The Bragg cross section for a given block does not depend on $\mathbf{k}_1$ and $\mathbf{k}_2$ separately; it depends on their difference - more exactly, on the vector $\mathbf{h}=\mathbf{k}_2-\mathbf{k}_1-\mathbf{H}$, where $\mathbf{H}$ is a reciprocal vector for this block. This cross section is given by

$$\sigma(\mathbf{h})=n^2|F|^2|\textstyle\int_v \exp(i\mathbf{hr})\,\mathrm{d}v|^2, \tag{2}$$

v being the volume of the perfect block. Let us denote by $\mathbf{H}_0$ the vector $\mathbf{H}$ for the most probable mosaic block. This vector together with the line connecting the centres of the sample and detector define the diffraction plane, considered horizontal. The wave vectors $\mathbf{k}_{10}$ and $\mathbf{k}_{20}$ lying in the horizontal plane and fulfilling exactly the Bragg condition $\mathbf{k}_{20}-\mathbf{k}_{10}=\mathbf{H}_0$ are the averages of the vectors $\mathbf{k}_1$ and $\mathbf{k}_2$ respectively. The vector $\mathbf{h}$ is determined only by the deviations from the averages of the vectors $\mathbf{k}_1$, $\mathbf{k}_2$, $\mathbf{H}$. These deviations can be easily written, if two new coordinate systems (see Fig. 1) are introduced: the oblique system $(\boldsymbol{\tau}_i)$ with $\boldsymbol{\tau}_1$, $\boldsymbol{\tau}_2$ lying in the horizontal plane and perpendicular to $\mathbf{i}_1$, $\mathbf{i}_2$ respectively, $\boldsymbol{\tau}_3=\mathbf{i}_3$; and the orthogonal system $(\mathbf{n}_i)$ with $\mathbf{n}_2$ along $\mathbf{H}_0$, $\mathbf{n}_1$ perpendicular to $\mathbf{H}_0$ in the horizontal plane and $\mathbf{n}_3=\mathbf{i}_3$. Then

$$\Delta\mathbf{k}_l=\Delta k\mathbf{i}_l+k_0\gamma_{lh}\boldsymbol{\tau}_l+k_0\gamma_{lv}\boldsymbol{\tau}_3,\quad (l=1,2), \tag{3a}$$

$$\Delta\mathbf{H}=\boldsymbol{\Delta}\times\mathbf{H}_0=2k_0\sin\theta(-\varepsilon_3\mathbf{n}_1+\varepsilon_1\mathbf{n}_3). \tag{3b}$$

Here θ is the Bragg angle, γ_{lh}, γ_{lv} $(l=1,2)$ are the horizontal (h) and vertical (v) divergence angles, $k_0=|\mathbf{k}_{10}|=|\mathbf{k}_{20}|=H/(2\sin\theta)$, $\Delta k=k_1-k_0=k_2-k_0$ and ε_i are the components of $\boldsymbol{\Delta}$ in the $(\mathbf{n}_i)$ system. Writing all the vectors in the $(\boldsymbol{\tau}_i)$ system, one obtains the vector $\mathbf{h}$ as follows:

$$\mathbf{h}=k_0[-(\Gamma_1-\varepsilon_3)\boldsymbol{\tau}_1+(\Gamma_2-\varepsilon_3)\boldsymbol{\tau}_2+(\Gamma_3-2\sin\theta\varepsilon_1)\boldsymbol{\tau}_3] \tag{4}$$

where Γ_i $(i=1,2,3)$ are defined as follows:

$$\begin{aligned}\Gamma_1&=\gamma_{1h}-\Delta k\tan\theta/k_0,\\ \Gamma_2&=\gamma_{2h}+\Delta k\tan\theta/k_0,\\ \Gamma&=\gamma_{2v}-\gamma_{1v}.\end{aligned} \tag{5}$$

The quantities Γ_i, chosen to give a unique treatment for both diffraction methods, are equivalent to divergence angles, though their nature is not purely angular (except for Γ_3). By convention we call them equivalent divergence angles. The average cross sections $\bar{\sigma}(\mathbf{k}_1\to\mathbf{k}_2)=\bar{\sigma}(\mathbf{k}_2\to\mathbf{k}_1)$ are then

$$\bar{\sigma}(\Gamma_1,\Gamma_2,\Gamma_3)=\iiint_{-\infty}^{\infty}\sigma(\Gamma_1-\varepsilon_3,\Gamma_2-\varepsilon_3,\Gamma_3-2\varepsilon_1\sin\theta)\times W(\varepsilon_1,\varepsilon_2,\varepsilon_3)\,\mathrm{d}\varepsilon_1\,\mathrm{d}\varepsilon_2\,\mathrm{d}\varepsilon_3. \tag{6}$$

The integrated cross sections $\int\mathrm{d}\mathbf{k}_2\,\bar{\sigma}(\mathbf{k}_1\to\mathbf{k}_2)$ and $\int\mathrm{d}\mathbf{k}_1\,\bar{\sigma}(\mathbf{k}_2\to\mathbf{k}_1)$ are in general different from each other and depend only on one equivalent divergence angle, Γ_1 and Γ_2 respectively. We denote them by $\bar{\sigma}_1(\Gamma_1)$ and $\bar{\sigma}_2(\Gamma_2)$.

Let us denote by P_i the integral of I_i over the vertical divergence angle γ_{iv} $(i=1,2)$. If $(1a)$ is integrated over γ_{1v} in the range $(-\infty,\infty)$, then the left-hand side and the first term of the right-hand side become $\partial P_1/\partial x_1$ and $-[\mu+\bar{\sigma}_1(\Gamma_1)]P_1$. In the second term of the right-hand side this integration acts only on the cross section $\bar{\sigma}(\Gamma_1,\Gamma_2,\Gamma_3)$ resulting in $\bar{\sigma}(\Gamma_1,\Gamma_2)$, a function independent of γ_{2v}; consequently, the existing integral over γ_{2v} acts only on I_2 and the second term becomes $\int_{-\infty}^{\infty}\mathrm{d}\gamma_{2h}\,\bar{\sigma}(\Gamma_1,\Gamma_2)P_2$. Evidently, here $\mathrm{d}\gamma_{2h}$ can be replaced by $\mathrm{d}\Gamma_2$. In the same manner we proceed with $(1b)$, inverting the roles of γ_{1v} and γ_{2v}. Thus we obtain two equations for the functions P_1,

P_2 similar to (1) except for the simple angular integral for the second term on the right-hand side. The cross section under this integral has the form

$$\bar{\sigma}(\Gamma_1, \Gamma_2) = \int_{-\infty}^{\infty} \mathrm{d}\varepsilon_3\, \sigma(\Gamma_1 - \varepsilon_3, \Gamma_2 - \varepsilon_3) W(\varepsilon_3) \quad (7a)$$

where

$$\sigma(\Gamma_1, \Gamma_2) = \int_{-\infty}^{\infty} \mathrm{d}\Gamma_3\, \sigma(\Gamma_1, \Gamma_2, \Gamma_3) \quad (7b)$$

$$W(\varepsilon_3) = \iint_{-\infty}^{\infty} \mathrm{d}\varepsilon_1\, \mathrm{d}\varepsilon_2\, W(\varepsilon_1, \varepsilon_2, \varepsilon_3). \quad (7c)$$

The formulae (7) are obtained by integrating (6) over Γ_3, an operation imposed by the integration of (1a) and (1b) over γ_{1v} and γ_{2v} respectively. The function $W(\varepsilon_3)$ is the one-dimensional mosaic distribution seen in a particular diffraction process and it is the projection on the axis $\mathbf{n}_3$ of the three-dimensional mosaic distribution $W(\boldsymbol{\Delta})$ (Nelmes, 1980). The integral cross sections $\bar{\sigma}_1(\Gamma_1)$ and $\bar{\sigma}_2(\Gamma_2)$ are found by integrating (7a) over Γ_2 and Γ_1 respectively. Formally, $\bar{\sigma}(\Gamma_1, \Gamma_2)$ can be factorized as follows:

$$\bar{\sigma}(\Gamma_1, \Gamma_2) = \bar{\sigma}_1(\Gamma_1) Z_1(\Gamma_1, \Gamma_2) = \bar{\sigma}_2(\Gamma_2) Z_2(\Gamma_2, \Gamma_1). \quad (8)$$

Hence, the classical energy transfer equations allowing one to obtain the secondary extinction factor both for angular dispersive and energy dispersive diffraction methods are the following:

$$\partial P_1(\mathbf{r}, \Gamma_1)/\partial x_1 = -[\mu + \bar{\sigma}_1(\Gamma_1)] P_1(\mathbf{r}, \Gamma_1) + \bar{\sigma}_1(\Gamma_1) \int_{-\infty}^{\infty} Z_1(\Gamma_1, \Gamma_2) P_2(\mathbf{r}, \Gamma_2)\, \mathrm{d}\Gamma_2 \quad (9a)$$

$$\partial P_2(\mathbf{r}, \Gamma_2)/\partial x_2 = -[\mu + \bar{\sigma}_2(\Gamma_2)] P_2(\mathbf{r}, \Gamma_2) + \bar{\sigma}_2(\Gamma_2) \int_{-\infty}^{\infty} Z_2(\Gamma_2, \Gamma_1) P_1(\mathbf{r}, \Gamma_1)\, \mathrm{d}\Gamma_1. \quad (9b)$$

The boundary conditions for the functions P_1 and P_2 are as simple as for the functions I_1 and I_2. Thus, if the crystal has a convex shape and is bathed by an incident beam with uniform spatial distribution of intensity, the boundary conditions are (see Fig. 2)

$$P_1(\mathbf{r}, \Gamma_1)|_{ABC} = 1; \qquad P_2(\mathbf{r}, \Gamma_2)|_{BCD} = 0. \quad (10a,b)$$

The equations (9) are different from HZ equations. Their right-hand sides contain angular integrals and different integrated cross sections $\bar{\sigma}_i(\Gamma_i)$. The existence of the integrals on the right-hand side of (9) is a direct consequence of the smallness of the mean mosaic block. The problem was first discussed by Darwin (1922) and later by Werner (1974) and others (see *e.g.* Suortti, 1982). If the mosaic block is small, the size of the corresponding reflecting domain in reciprocal space is large. The effect of the mosaic misorientation is to extend the reflecting domain perpendicularly to the vector $\mathbf{H}_0$. Thus if a well collimated monochromatic beam is diffracted, the reflected beam becomes divergent. This divergence is determined by the section cut from the reflecting domain by the Ewald sphere. The successive reflexions make both incident and diffracted beams divergent; thus to write correctly the feedback term in the transfer equations we have to perform an integration over the divergence angle. If, moreover, the mean mosaic block has an anisotropic shape, the corresponding reflecting domain is ellipsoidal rather than spherical. Consequently the divergences of the incident and diffracted beams as well as the integrated cross sections $\bar{\sigma}_1$ and $\bar{\sigma}_2$ are different from each other (because the sections cut by the Ewald sphere are different). These effects become negligibly small for type I crystals. Indeed, if the mosaic width is much greater than the natural width, the reflecting domain is very flattened and the section cut by the Ewald sphere is small. Consequently (see § 4 below) the functions Z_1 and Z_2 become $\delta(\Gamma_1 - \Gamma_2)$, $\bar{\sigma}_1$ and $\bar{\sigma}_2$ become identical and (9) are reduced to HZ equations.

3. The solution of the transfer equations and the general expression for the extinction factor

By definition, the extinction factor y is the ratio between the diffracted integral intensity and its kinematical approximation. If the sample is totally immersed in the incident beam, then from Fig. 2 we have

$$y = [\sin 2\theta / QVA(\mu)] \times \int_{-\infty}^{\infty} \mathrm{d}\Gamma_2 \int \mathrm{d}x_3 \int_{x_1(B)}^{x_1(D)} \mathrm{d}x_1 P_2[x_1, x_2^1(x_1), x_3, \Gamma_2]. \quad (11)$$

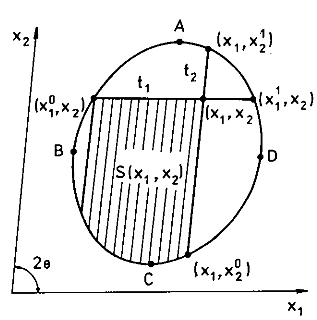

Fig. 2. The cross section of the crystal in a plane parallel to the diffraction plane. The hatched area $S(x_1, x_2)$ is the integration area for equations (20), (28).

Here V is the sample's volume and the quantities Q, $A(\mu)$ are

$$Q = n^2|F|^2\lambda^3/\sin 2\theta, \tag{12}$$

$$A(\mu) = V^{-1}\int_V \mathrm{d}V \exp[-\mu(t_1+t_2)], \tag{13}$$

where t_1, t_2 represent the path in the sample of the incident and diffracted beams, respectively:

$$t_1(x_1, x_2) = x_1 - x_1^0(x_2), \tag{14a}$$

$$t_2(x_1, x_2) = x_2^1(x_1) - x_2. \tag{14b}$$

As the problem is a plane one, in the following we will omit x_3. The diffracted intensity P_2 in (11) is found by solving (9) under the boundary conditions (10). This can be done for any form of the functions $\bar{\sigma}_i(\Gamma_i)$ and $Z_i(\Gamma_i, \Gamma_j)$. The strategy is the same as in Becker & Coppens (1974*a*), but the calculation here is longer and for the sake of brevity some elementary but tiresome details are skipped.

In the first stage (9) and (20) are transformed into an integral equation. To do that let us define the functions ψ_i and $\xi^{(i)}$ as follows:

$$P_i(x_1, x_2, \Gamma_i) = \psi_i(x_1, x_2, \Gamma_i)\exp[-\mu(x_1+x_2)] \quad (i=1,2); \tag{15}$$

$$\xi^{(i)}(x_1, x_2, \Gamma_i) = \int_{-\infty}^{\infty} Z_i(\Gamma_i, \Gamma_j)\psi_j(x_1, x_2, \Gamma_j)\,\mathrm{d}\Gamma_j \quad (i \neq j = 1,2). \tag{16}$$

Then (9) and the boundary conditions (10) become

$$\begin{aligned}\partial\psi_i(x_1, x_2, \Gamma_i)/\partial x_i = {} & -\bar{\sigma}_i(\Gamma_i)\psi_i(x_1, x_2, \Gamma_i)\\ & +\bar{\sigma}_i(\Gamma_i)\xi^{(i)}(x_1, x_2, \Gamma_i) \quad (i=1,2);\end{aligned} \tag{17}$$

$$\psi_1(x_1^0, x_2) = \exp[\mu(x_1^0+x_2)] = g(x_2) \tag{18a}$$

$$\psi_2(x_1, x_2^0) = 0. \tag{18b}$$

The equations (17) under the boundary conditions (18) are solved as inhomogeneous differential equations and give the result

$$\begin{aligned}\psi_1(x_1, x_2, \Gamma_1) = {} & g(x_2)\exp[-\bar{\sigma}_1(\Gamma_1)t_1(x_1, x_2)]\\ & +\bar{\sigma}_1(\Gamma_1)\int_{x_1^0}^{x_1}\exp[-\bar{\sigma}_1(\Gamma_1)(x_1-u_1)]\\ & \times\xi^{(1)}(u_1, x_2, \Gamma_1)\,\mathrm{d}u_1,\end{aligned} \tag{19a}$$

$$\begin{aligned}\psi_2(x_1, x_2, \Gamma_2) = {} & \bar{\sigma}_2(\Gamma_2)\int_{x_2^0}^{x_2}\exp[-\bar{\sigma}_2(\Gamma_2)(x_2-u_2)]\\ & \times\xi^{(2)}(x_1, u_2, \Gamma_2)\,\mathrm{d}u_2.\end{aligned} \tag{19b}$$

Now, multiplying (19*a*) by $Z_2(\Gamma_2, \Gamma_1)$, (19*b*) by $Z_1(\Gamma_1, \Gamma_2)$ and integrating over Γ_1 and Γ_2, respectively, one obtains two coupled integral equations for the functions $\xi^{(i)}$. Eliminating $\xi^{(1)}$ one obtains

$$\begin{aligned}\xi^{(2)}(x_1, x_2, \Gamma_2) = {} & g(x_2)\int_{-\infty}^{\infty}\mathrm{d}\Gamma_1\, Z_2(\Gamma_1, \Gamma_1)\\ & \times\exp[-\bar{\sigma}_1(\Gamma_1)t_1(x_1, x_2)]\\ & +\int_{-\infty}^{\infty}\mathrm{d}\Gamma_1\, Z_2(\Gamma_2, \Gamma_1)\bar{\sigma}_1(\Gamma_1)\\ & \times\int_{-\infty}^{\infty}\mathrm{d}\Lambda_2\, Z_1(\Gamma_1, \Lambda_2)\bar{\sigma}_2(\Lambda_2)\\ & \times\int_{x_1^0}^{x_1}\mathrm{d}u_1\int_{x_2^0}^{x_2}\mathrm{d}u_2\exp[-\bar{\sigma}_1(\Gamma_1)(x_1-u_1)\\ & -\bar{\sigma}_2(\Lambda_2)(x_2-u_2)]\xi^{(2)}(u_1, u_2, \Lambda_2).\end{aligned} \tag{20}$$

The extinction factor can be expressed by the function $\xi^{(2)}$; indeed, from (15) and (19*b*), (11) becomes

$$\begin{aligned}y = {} & [QVA(\mu)]^{-1}\int_{-\infty}^{\infty}\mathrm{d}\Gamma_2\,\bar{\sigma}_2(\Gamma_2)\int\mathrm{d}x_3\int_{S_0(x_3)}\mathrm{d}S f(x_1)\\ & \times\exp[-\bar{\sigma}_2(\Gamma_2)t_2(x_1, x_2)]\xi^{(2)}(x_1, x_2, \Gamma_2)\end{aligned} \tag{21}$$

where we have denoted by $S_0(x_3)$ the crystal cross-sectional area for a given x_3 and by $f(x_1)$ the function

$$f(x_1) = \exp[-\mu(x_1+x_2^1)]. \tag{22}$$

In the second stage, the integral equation (20) is solved by successive approximations. For that, the following factorization for $\bar{\sigma}_i$ and series development of $\xi^{(2)}$ are necessary:

$$\bar{\sigma}_i(\Gamma_i) = QG_i(\Gamma_i) \tag{23}$$

$$\xi^{(2)}(x_1, x_2, \Gamma_2) = \sum_{n=0}^{\infty}[(-1)^n/n!]\,\xi_n(x_1, x_2, \Gamma_2)Q^n. \tag{24}$$

Here the functions G_i and ξ_n do not depend on Q. Introducing (23), (24) into (20) and identifying the coefficients of Q^n, one obtains

$$\begin{aligned}\xi_n(x_1, x_2, \Gamma_2) = {} & F_n(\Gamma_2)g(x_2)t_1^n(x_1, x_2)\\ & +n(n-1)\sum_{l=0}^{n-2}\sum_{m=0}^{l}\binom{n-2}{l}\binom{l}{m}\\ & \times\int_{-\infty}^{\infty}\mathrm{d}\Lambda_2\, H_{n-1-l}(\Gamma_2, \Lambda_2)\\ & \times G_2^{l-m+1}(\Lambda_2)\\ & \times\int_{S(x_1,x_2)}\mathrm{d}u_1\,\mathrm{d}u_2\,(x_1-u_1)^{n-2-l}\\ & \times(x_2-u_x)^{l-m}\xi_m(u_1, u_2, \Lambda_2),\end{aligned} \tag{25}$$

where we have denoted by $S(x_1, x_2)$ the hatched area in Fig. 2 and by F_n and H_{n+1} the following functions:

$$F_n(\Gamma_2) = \int_{-\infty}^{\infty} \mathrm{d}\Gamma_1 Z_2(\Gamma_2, \Gamma_1) G_1^n(\Gamma_1); \quad (n \geq 0), \tag{26}$$

$$H_{n+1}(\Gamma_2, \Lambda_2) = \int_{-\infty}^{\infty} \mathrm{d}\Gamma_1\, Z_2(\Gamma_2, \Gamma_1) \times G_1^{n+1}(\Gamma_1) Z_1(\Gamma_1, \Lambda_2); \quad (n \geq 0). \tag{27}$$

In (25) and below, the sum exists only if the upper limit is greater than or equal to the lower one.

The recurrence relation (25) can be solved using the BC approximation presented in Appendix *A*. Indeed, let us iterate (25) beginning with $n=0$. ξ_0 and ξ_1 are simple functions [first term of (25)]; ξ_2 and ξ_3 contain an angular and a surface integral. But ξ_4 contains a double angular and a double surface integral (*A*1). The latter is reduced to a simple surface integral using the BC approximation (*A*4). If one continues with ξ_5 and ξ_6 in the same manner, enough information is obtained to suggest the following form for the general term ξ_n:

$$\begin{aligned}\xi_n(x_1, x_2, \Gamma_2) = {} & F_n(\Gamma_2) g(x_2) t_1^n(x_1, x_2) + n(n-1) \int_{S(x_1,x_2)} \mathrm{d}u_1\, \mathrm{d}u_2\, g(u_2) \\ & \times \sum_{m=0}^{n-2} t_1^m(u_1, u_2) \times \sum_{l=m}^{n-2} \binom{n-2}{l} \binom{l}{m} (x_1 - u_1)^{n-2-l} \\ & \times (x_2 - u_2)^{l-m} K_{n-2,m,l}(\Gamma_2),\end{aligned} \tag{28}$$

where the functions $K(\Gamma_2)$ fulfil the following recurrence relations ($n \geq 2$):

$$K_{n-2,m,l}(\Gamma_2) = \int_{-\infty}^{\infty} \mathrm{d}\Lambda_2\, H_{n-1-l}(\Gamma_2, \Lambda_2) V_{lm}(\Lambda_2) \tag{29a}$$

$$\begin{aligned}V_{lm}(\Gamma_2) = {} & G_2^{l-m+1}(\Gamma_2) F_m(\Gamma_2) + \sum_{j=m+1}^{l} G_2^{l-j+1}(\Gamma_2) \\ & \times \sum_{k=0}^{m-1} K_{j-2,k,j-m+k-1}(\Gamma_2).\end{aligned} \tag{29b}$$

The correctness of (28) is verified in the last step of this complete induction procedure by replacing it in (25) and using once again the BC approximation (*A*4). Now, if (21) is developed in a power series of Q and ξ_n is replaced by (28), another double surface integral (*A*5) is obtained, which is reduced to a simple surface integral using the BC approximation (*A*6). Finally one obtains

$$\begin{aligned}y = {} & [VA(\mu)]^{-1} \int_{-\infty}^{\infty} \mathrm{d}\Gamma_2 \int_V \mathrm{d}V \exp[-\mu(t_1 + t_2)] \\ & \times \sum_{n=0}^{\infty} \frac{(-1)^n}{n!} Q^n \sum_{m=0}^{n} \binom{n}{m} V_{nm}(\Gamma_2) t_1^m t_2^{n-m}\end{aligned} \tag{30}$$

where the functions $V_{nm}(\Gamma_2)$ satisfy a recurrence relation obtained from (29):

$$\begin{aligned}V_{nm}(\Gamma_2) = {} & G_2^{n-m+1}(\Gamma_2) F_m(\Gamma_2) + \sum_{j=m+1}^{n} G_2^{n-j+1}(\Gamma_2) \sum_{l=0}^{m-1} \int_{-\infty}^{\infty} \mathrm{d}\Lambda_2 \\ & \times H_{l+1}(\Gamma_2, \Lambda_2) V_{j-2-l,m-l-1}.\end{aligned} \tag{31}$$

The formula (30) is the most general expression for the extinction factor in the limits of the transfer theory and BC approximation, being valid for any model of the crystal microstructure. For practical purposes a closed formula must be obtained. This is a simple task if the crystal is of type I, but for the general type we need one more approximation. In the following the calculations will be much simplified if the mosaic model is introduced explicitly.

4. Extinction for definite mosaic distributions

Traditionally, the misorientation of the mosaic is described by the Gaussian distribution which in three dimensions is

$$W(\boldsymbol{\Delta}) = g_1 g_2 g_3 \exp\left(-\pi \sum_i g_i^2 \Delta_i^2\right). \tag{32}$$

Here the variables Δ_i are small rotations around the principal axes of the constant probability ellipsoid and g_i give the widths of the distribution at half height:

$$w_i = 2(\ln 2/\pi)^{1/2}/g_i = 0{\cdot}939/g_i.$$

The principal axes are oriented along the unit vectors $\mathbf{m}_i$ and in order to write down the distribution in the $(\mathbf{n}_i)$ system an orthogonal matrix $\mathsf{E}^{(m)}$ connecting $\mathbf{m}_i$ and $\mathbf{n}_i$ must be introduced:

$$\mathbf{m}_i = \sum_i E_{ij}^{(m)} \mathbf{n}_j \quad (i = 1, 2, 3). \tag{33}$$

With

$$\boldsymbol{\Delta} = \sum_i \Delta_i \mathbf{m}_i = \sum_i \varepsilon_i \mathbf{n}_i$$

one obtains

$$W(\varepsilon_1, \varepsilon_2, \varepsilon_3) = |\mathsf{C}|^{1/2} \exp\left(-\pi \sum_j \sum_k C_{jk} \varepsilon_j \varepsilon_k\right), \tag{34}$$

$$\mathsf{C} = \mathsf{E}^{(m)\prime} \mathsf{G}^2 \mathsf{E}^{(m)}; \quad G_{ij} = g_i \delta_{ij}, \tag{35a,b}$$

where δ_{ij} are Kronecker symbols. By integrating over ε_1 and ε_2 one obtains the one-dimensional mosaic distribution seen in the diffraction process:

$$W(\varepsilon_3) = g_G \exp(-\pi g_G^2 \varepsilon_3^2), \quad (36)$$

$$1/g_G^2 = \sum_k E_{k3}^{(m)2}/g_k^2 \quad (37)$$

which must be convoluted with the unit-volume cross section $\sigma(\Gamma_1, \Gamma_2)$ of the average perfect block.

The latter is calculated in Appendix B (B12, B13) for an ellipsoid with principal axes r_i oriented along the unit vectors $\mathbf{c}_i$ $(i=1,2,3)$ and depends on the ellipsoid radii ρ_1, ρ_2 along the incident and diffracted directions respectively, and on the transformed Bragg angle θ' (when the ellipsoid is transformed into a sphere). These quantities can be calculated if the orthogonal matrix $\mathsf{E}^{(c)}$ relating the systems $(\mathbf{c}_i)$ and $(\mathbf{n}_i)$ is introduced:

$$\mathbf{c}_i = \sum_j E_{ij}^{(c)} \mathbf{n}_j \quad (i=1,2,3). \quad (38)$$

Indeed, using the transformation (see Fig. 1)

$$\mathbf{i}_l = \cos\theta \mathbf{n}_1 + (-1)^l \sin\theta \mathbf{n}_2 \quad (l=1,2) \quad (39)$$

and (C1), (C2) from Appendix C we have

$$1/\rho_l^2 = \sum_k [\cos\theta E_{k1}^{(c)} + (-1)^l \sin\theta E_{k2}^{(c)}]^2/r_k^2 \quad (l=1,2); \quad (40)$$

$$\cos 2\theta' = \rho_1\rho_2 \sum_k (\cos^2\theta E_{k1}^{(c)2} - \sin^2\theta E_{k2}^{(c)})/r_k^2. \quad (41)$$

Now the convolution (7) can be performed; with the factorizations (8) and (23) one obtains

$$G_i(\Gamma_i) = \alpha_{iG} \exp(-\pi\alpha_{iG}^2\Gamma_i^2) \quad (i=1,2), \quad (42)$$

$$Z_i(\Gamma_i, \Gamma_j) = (\alpha_{iG}/\delta_{iG}) \exp[-\pi(\alpha_{iG}^2/\delta_{iG}^2) \times (\nu_{iG}\Gamma_i - \Gamma_j)^2] \quad (i \neq j = 1,2), \quad (43)$$

where

$$\alpha_{iG}^2 = (g_G^2 c_0^2 \rho_j^2 \sin^2 2\theta/\lambda^2)/(g_G^2 + c_0^2\rho_j^2 \sin^2 2\theta/\lambda^2) \quad (i \neq j = 1,2), \quad (44)$$

$$\nu_{iG} = (g_G^2 \cos 2\theta' \rho_j/\rho_i + c_0^2\rho_j^2 \sin^2 2\theta/\lambda^2) \times (g_G^2 + c_0^2\rho_j^2 \sin^2 2\theta/\lambda^2)^{-1} \quad (i \neq j = 1,2), \quad (45)$$

$$\delta_{1G}^2 = 1/a_G^2 - \nu_{1G}^2, \qquad \delta_{2G}^2 = a_G^2 - \nu_{2G}^2. \quad (46a,b)$$

Here $c_0 = 1{\cdot}612$ and a_G is the block-shape-anisotropy parameter defined as

$$a_G = \alpha_{2G}/\alpha_{1G} = (\rho_1/\rho_2)[(g_G^2 + c_0^2\rho_2^2 \sin^2 2\theta/\lambda^2) \times (g_G^2 + c_0^2\rho_1^2 \sin^2 2\theta/\lambda^2)^{-1}]^{1/2}. \quad (47)$$

The following supplementary relations hold:

$$\nu_{2G} = a_G^2 \nu_{1G}; \qquad \delta_{2G} = a_G^2 \delta_{1G} \quad (48a,b)$$

$$\nu_{1G}\nu_{2G} + \delta_{1G}\delta_{2G} = 1. \quad (48c)$$

Always, $0 \leq \nu_{1G}\nu_{2G} \leq 1$ and consequently $0 \leq \delta_{1G}\delta_{2G} \leq 1$.

Let us now discuss the limiting situations. If $g_G \ll c_0 \sin 2\theta \min(\rho_1, \rho_2)/\lambda$, then $a_G = 1$, $\alpha_{1G} = \alpha_{2G} = g_G$, $\nu_{1G} = \nu_{2G} = 1$, $\delta_{1G} = \delta_{2G} = 0$, $\alpha_{iG}/\delta_{iG} \to \infty$ and as a consequence the functions Z_i are δ functions. In this situation the crystal is of type I, the extinction is governed by the mosaic only and the transfer equations are HZ. If, on the contrary, $g_G \gg c_0 \sin 2\theta \max(\rho_1, \rho_2)/\lambda$, then $a_G = \rho_1/\rho_2 \neq 1$, $\alpha_{iG} = c_0\rho_j \sin 2\theta/\lambda$, $\nu_{iG} = \rho_j \cos 2\theta'/\rho_i$, $\delta_{iG} = \rho_j \sin 2\theta'/\rho_i$, $(i \neq j = 1,2)$; α_{iG}/δ_{iG} are finite and Z_i are not δ functions. In this case the crystal is of type II, the extinction is governed only by the block size and the transfer equations are no longer HZ, as in the intermediate situation where the crystal is of mixed type. If $\sin 2\theta$ is very small, the crystal cannot be of pure type I; but in this case $\rho_1 \simeq \rho_2$, hence $a_G \simeq 1$, $\nu_{1G} = \nu_{2G} \simeq 1$, $\delta_{1G} = \delta_{2G} \simeq 0$ and although the crystal is of the mixed type the transfer equations are HZ. It is seen that when the quantity $(\delta_1\delta_2)_G$ is zero the transfer equations are always HZ and the extinction is correctly given by the BC theory. This parameter is directly obtained from (45) and (48c):

$$(\delta_1\delta_2)_G = g_G^2[g_G^2 \sin^2 2\theta' + c_0^2 \sin^2 2\theta \times (\rho_1^2 + \rho_2^2 - 2\rho_1\rho_2 \cos 2\theta')/\lambda^2] \times [(g_G^2 + c_0^2 \sin^2 2\theta \rho_1^2/\lambda^2) \times (g_G^2 + c_0^2 \sin^2 2\theta \rho_2^2/\lambda^2)]^{-1}. \quad (49)$$

Once given G_i and Z_i, it is possible to calculate the functions $V_{nm}(\Gamma_2)$. If (31) is iterated beginning with $n=0$, after a few steps it will be observed that every $V_{nm}(\Gamma_2)$ is a sum of $\binom{n}{m}$ Gaussians, all having the common factor $\alpha_{1G}^m \alpha_{2G}^{n-m+1}$. For type I crystals all the terms are identical and

$$V_{nm}(\Gamma_2) = \binom{n}{m} W^{n+1}(\Gamma_2) = \binom{n}{m} g_G^{n+1} \exp[-\pi(n+1)g_G^2\Gamma_2^2]. \quad (50)$$

For the general-type crystal the expected difficulties in finding exact $V_{nm}(\Gamma_2)$ are discouraging. On the other hand, we do not need the profile but the integral of $V_{nm}(\Gamma_2)$, and so we accept the following approximation suggested by (50):

$$V_{nm}(\Gamma_2) = \binom{n}{m} \alpha_{1G}^m \alpha_{2G}^{n-m+1} p_{nm} \times \exp[-\pi(n+1)\alpha_{2G}^2(p_{nm}/v_{nm})^2\Gamma_2^2]. \quad (51)$$

Introducing this into (31) and retaining only (a) the height and area or (b) the height and the second moment, we obtain two coupled recurrence relations for the coefficients p_{nm} and v_{nm}. These relations depend on one parameter only, $(\delta_1\delta_2)_G$, and can be solved numerically. The quantities of interest [which determine the areas of $V_{nm}(\Gamma_2)$] are v_{nm}. They fulfil the conditions $v_{nm}=v_{n,n-m}$ and $v_{nm}\le 1$, the equality taking place for $m=0$ and $m=n$ (and of course always for $\delta_1\delta_2=0$). The recurrence relations (a) overestimate v_{nm} and, conversely, (b) underestimate them. Some coefficients v_{nm} calculated for $(\delta_1\delta_2)_G=1$ are represented in Fig. 3.

With the approximation (51) the extinction factor (30) becomes

$$y=\sum_{n=0}^{\infty}[(-1)^n/n!][(Q\alpha_{1G})^n/(n+1)^{1/2}]\overline{t^{(n)}}, \quad (52a)$$

$$\overline{t^{(n)}}=[VA(\mu)]^{-1}\int_V \mathrm{d}V\exp[-\mu(t_1+t_2)]$$
$$\times\sum_{m=0}^{n}\binom{n}{m}^2 v_{nm}t_1^m(a_Gt_2)^{n-m}. \quad (52b)$$

This differs from the corresponding Becker & Coppens (1974a) result [their equation (51)] by the coefficients v_{nm} and a_G in $t^{(n)}$. The coefficient a_G occurs in (52) for $n\ge 1$, then it occurs also in the main extinction parameter. As in BC this parameter is defined by (only the factor 2/3 is ignored)

$$x=Q\alpha_{1G}\overline{t^{(1)}}. \quad (53)$$

The quantity $\overline{t^{(1)}}$ here is the mean path in the crystal [or in the mosaic block if V in (52b) is replaced by v] only for $a_G=1$.

The coefficients v_{nm} occur in (52) only for $n\ge 2$ and they give a relatively small correction for the BC formula compared with a_G. To evaluate this correction we have calculated y by direct summation of (52) for a crystal of parallelepipedic shape with the edges along x_1, x_2, x_3, $\mu=0$ and $a_G=1$. In this case the volume integral in (52b) is readily performed. v_{nm} were calculated numerically for $\delta_1\delta_2=0$, 0·4, 0·7, 1·0

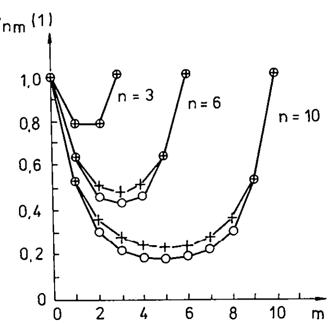

Fig. 3. Some of the coefficients v_{nm} calculated for $\delta_1\delta_2=1$; $+v_{nm}$ overestimated; ○ v_{nm} underestimated.

and $n\le 60$. For these n it is possible to sum (52a) with an accuracy of three decimal digits in the range $0\le x\le 5{\cdot}7$ ($y\ge 0{\cdot}2$). The results of the summations made with underestimated and overestimated v_{nm} differ from each other by at most 1·1%, therefore their mean value was considered satisfactory. The values of y calculated in this way for values of x varied with a step of 0·1 were used to fit the following empirical function:

$$y(x,\delta_1\delta_2)=y_0(x)[1-\delta_1\delta_2A_0x^{C_0}/(1+B_0x^{C_0})], \quad (54)$$

where $y_0(x)=y(x,0)$. We have obtained $A_0=0{\cdot}02$, $B_0=0{\cdot}26$, $C_0=1{\cdot}5$ with

$$R=\sum|y(\mathrm{calc.})-y(x,\delta_1\delta_2)|/\sum y(\mathrm{calc.})=0{\cdot}008.$$

For $x\le 30$ the maximum deviation of $y(x,1)$ from $y_0(x)$ is only 8%. This explains why the BC formula gives good results in many cases.

For the crystal with $\mu\ne 0$, $a\ne 1$ and of other shape or mosaic distribution, small variations of the parameters A_0, B_0 and C_0 are expected. But if the smallness of the correction (54) itself is taken into account, these variations can be neglected. If (54) is in general accepted, it only remains to express y_0. For that we must take $v_{nm}=1$ in (52b). But in this case, by using the identity

$$\sum_{n=0}^{\infty}\frac{(-1)^n}{n!}c^n\sum_{m=0}^{n}\binom{n}{m}^2u^mv^{n-m}$$
$$=\exp[-c(u+v)]I_0[2c(uv)^{1/2}], \quad (55)$$

where I_0 is the modified Bessel function, one obtains y_0 as follows:

$$y_0=[QVA(\mu)]^{-1}\int_V\mathrm{d}V\exp[-\mu(t_1+t_2)]$$
$$\times\int_{-\infty}^{\infty}\mathrm{d}\gamma\,\bar\sigma_1(\gamma)\exp[-\bar\sigma_1(\gamma)(t_1+at_2)]$$
$$\times I_0[2\bar\sigma_1(\gamma)(at_1t_2)^{1/2}]. \quad (56)$$

This expression is valid for all mosaic distributions leading to the functions $V_{nm}(\Gamma_2)$, in which the quantity $\alpha_1^m\alpha_2^{n-m+1}$ can be factorized.

It seems ($e.g.$ Becker & Coppens, 1974b) that the Lorentz mosaic distribution is more adequate for the secondary extinction than the Gauss distribution. But it must be noted that a three-dimensional Lorentz function has an infinite norm and cannot be a physical distribution. A function with tails longer than Gaussian which may be a mosaic distribution is

$$W(\mathbf{\Delta})=2\pi g_1g_2g_3/\left[1+\beta_0\left(\sum_i g_i^2\Delta_i^2\right)^m\right], \quad (m\ge 2), \quad (57)$$

where $\beta_0(m)$ results from the normalization condition. Taking $m=2$ we obtain $\beta_0=4\pi^4$ and $w_i=2^{1/2}/(\pi g_i)=0{\cdot}45/g_i$. The one-dimensional mosaic distribution becomes

$$W(\varepsilon_3)=(\pi g'_L/2)[1-(2/\pi)\arctan 2\pi^2 g'^2_L\varepsilon_3^2], \quad (58)$$

where for g'_L one has exactly the same expression as for g_G. The asymptotic behaviour is ε_3^{-2}, when it can be well approximated by the Lorentz function:

$$W(\varepsilon_3)=g_L/(1+\pi^2 g_L^2\varepsilon_3^2) \quad g_L=\pi g'_L/2. \quad (59)$$

This is the sole argument for preserving the name Lorentz for this distribution. Further, to calculate the functions $G_i(\Gamma_i)$ it is enough [because (54) is accepted] to convolute (59) with the perfect block cross sections $\sigma_i(\Gamma_i)$ given by (B14). Their Lorentzian approximations (B16) are preferable for reasons of simplicity and the following results:

$$G_i(\Gamma_i)=\alpha_{iL}/(1+\pi^2\alpha_{iL}^2\Gamma_i^2) \quad (i=1,2); \quad (60)$$

$$\alpha_{iL}=(1\cdot5 g_L\rho_j\sin 2\theta/\lambda)/(g_L+1\cdot5\rho_j\sin 2\theta/\lambda) \quad (i\neq j=1,2). \quad (61)$$

The block anisotropy parameter a_L becomes

$$\begin{aligned}a_L&=\alpha_{2L}/\alpha_{1L}\\&=(\rho_1/\rho_2)(g_L+1\cdot5\rho_2\sin 2\theta/\lambda)\\&\quad\times(g_L+1\cdot5\rho_1\sin 2\theta/\lambda)^{-1}\end{aligned} \quad (62)$$

and, in place of (49),

$$\begin{aligned}(\delta_1\delta_2)_L^{1/2}&=g_L[g_L\sin 2\theta'+1\cdot5\sin 2\theta(\rho_1^2+\rho_2^2\\&\quad-2\rho_1\rho_2-2\rho_1\rho_2\cos 2\theta')^{1/2}/\lambda]\\&\quad\times[(g_L+1\cdot5\rho_1\sin 2\theta/\lambda)\\&\quad\times(g_L+1\cdot5\rho_2\sin 2\theta/\lambda)]^{-1}\end{aligned} \quad (63)$$

is used.

It can be anticipated that if the crystal is nearly type II the Gaussian variant will work badly, because here $\bar\sigma_i(\Gamma_i)$ is practically given by $\sigma_i(\Gamma_i)$, roughly approximated by a Gaussian.

5. Application to spherical and ellipsoidal crystals

The diffraction data for precise structure determination are collected on spherical crystals, because this shape makes it relatively easy to make absorption and extinction corrections. For extinction, polyhedral crystals may be approximated by ellipsoids. If one denotes by ρ_{10} and ρ_{20} the ellipsoid radii along $\mathbf{i}_1$ and $\mathbf{i}_2$ and transforms the ellipsoid into a sphere of unit radius (when θ is transformed into θ'_0), (53), (56) become

$$x=Q(\alpha_1\alpha_2\rho_{10}\rho_{20})^{1/2}\overline{t'(a_0,a_e)} \quad (64)$$

$$\begin{aligned}y_0&=[3/4\pi A(\zeta,a_0)]\int_{-\infty}^{\infty}\mathrm{d}\gamma\,\varphi(\gamma)\\&\quad\times\int_{S_1}\mathrm{d}V'\exp[-\zeta(t'_1a_0^{1/2}+t'_2/a_0^{1/2})]\\&\quad\times\exp\left[-x\varphi(\gamma)\frac{t'_1a_e^{1/2}+t'_2/a_e^{1/2}}{\overline{t'(a_0,a_e)}}\right]\\&\quad\times I_0\left[2x\varphi(\gamma)\frac{(t'_1t'_2)^{1/2}}{\overline{t'(a_0,a_e)}}\right]\end{aligned} \quad (65)$$

where S_1 is the sphere of unit radius and ζ, $A(\zeta,a_0)$, $\overline{t'(a_0,a_e)}$ are given by

$$\zeta=\mu(\rho_{10}\rho_{20})^{1/2}; \quad (66a)$$

$$A(\zeta,a_0)=\frac{3}{4\pi}\int_{S_1}\mathrm{d}V'\exp[-\zeta(t'_1a_0^{1/2}+t'_2/a_0^{1/2})] \quad (66b)$$

$$\begin{aligned}\overline{t'(a_0,a_e)}&=\frac{3}{4\pi A(\zeta,a_0)}\int_{S_1}\mathrm{d}V'(t'_1a_e^{1/2}+t'_2/a_e^{1/2})\\&\quad\times\exp[-\zeta(t'_1a_0^{1/2}+t'_2/a_0^{1/2})].\end{aligned} \quad (67)$$

We have denoted by $\varphi(\gamma)$ one of the functions $\exp(-\pi\gamma^2)$ or $(1+\pi^2\gamma^2)^{-1}$ and by a_0, a_e two anisotropy parameters:

$$a_0=\rho_{10}/\rho_{20}; \qquad a_e=a_0/a. \quad (68a,b)$$

The former gives the crystal-shape anisotropy and is related only to absorption; the latter is related to scattering and contains all the anisotropies in the crystal: mosaic, block-shape and crystal-shape anisotropy. Let us call a_e the effective anisotropy.

To calculate the extinction factor in the structure-refinement programs an empirical formula is used, reproducing numerically the exact expression. From (65) it is seen that y_0 for the secondary extinction contains five parameters: x, θ, ζ, a_0 and a_e. The dependence on ζ, a_0 and a_e is of two kinds: an explicit dependence and an implicit one through the parameter x. The former is weaker than the latter and can be neglected for small ζ and for a_0, a_e near 1. If these conditions are not fulfilled, the approximation could be rough. On the other hand, searching for an empirical formula with five variables requires much computational time and a large memory which may be difficult to achieve with small computers; in this case the variables are restricted to four.

For spherical crystals ($a_0=1$) we have computed y_0 with (65) at 4592 points in the volume: $0\le x\le 30$, $0\cdot05\le\eta\le 0\cdot95$, $0\le\zeta\le 3$ and $1\le a\le 8$, where $\eta=\sin\theta$. A Gaussian integration grid was used providing an accuracy of three decimal digits in y_0. With $\chi=\ln a$, the following empirical function was fitted by the least-squares method with values computed from (65):

$$\begin{aligned}y_0(x,\eta,\zeta,\chi)&=y_{00}(x,\eta)[1+\zeta A_2x^{1\cdot5}/(1+B_2x^{1\cdot5})]\\&\quad\times\left[1-\frac{\chi^2A_3x^{1\cdot5}/(1+B_3x^{1\cdot5})}{1+\chi^2C_3x^{1\cdot5}/(1+D_3x^{1\cdot5})}\right],\end{aligned} \quad (69)$$

the coefficients $A_2, \ldots, D_3$ being polynomials in η and ζ. For the function $y_{00}(x, \eta)$ we have tried the formula proposed by Becker & Coppens (1974*a*) and found that some values are reproduced with an error up to 10%, though the R factor (for the fit of y_{00} only) is good. Then we modified the BC empirical formula as follows (for Gauss and Lorentz distributions):

$$y_{00}^{(G)}(x, \eta) = \left[1 + x\left(D_1 + \frac{A_1 x^{C_1}}{1 + B_1 x^{C_1}}\right)\right]^{-1/2}; \quad D_1 = 2^{1/2}, \tag{70}$$

$$y_{00}^{(L)}(x, \eta) = \left[1 + x\left(D_1 + \frac{A_1 x}{1 + B_1 x} + \frac{C_1 x^2}{(1 + B_1 x)^2}\right)\right]^{-1/2}; \quad D_1 = 1, \tag{71}$$

the coefficients A_1, B_1, C_1 being polynomials in η. The expressions for the coefficients $A_1, \ldots, D_3$ obtained from the fit are

(*a*) *for the Gauss mosaic*:

$$\begin{aligned} A_1 &= 0{\cdot}721 + 0{\cdot}12\eta - 0{\cdot}736\eta^2 \\ 10B_1 &= 0{\cdot}11 + 0{\cdot}603\eta - 0{\cdot}709\eta^2 \\ C_1 &= 1 - 0{\cdot}505\eta^2 \\ 10A_2 &= 0{\cdot}08 + 0{\cdot}877\eta - 0{\cdot}577\eta^2 - 0{\cdot}068\eta\zeta \\ B_2 &= 0{\cdot}502 - 0{\cdot}912\eta - 0{\cdot}15\zeta + 0{\cdot}734\eta^2 \\ &\quad + 0{\cdot}138\eta\zeta + 0{\cdot}021\zeta^2 \\ 10A_3 &= (0{\cdot}124 + 0{\cdot}082\eta - 0{\cdot}031\zeta)\eta^2 \\ 10B_3 &= 0{\cdot}338 + 0{\cdot}094\eta - 0{\cdot}062\zeta \\ 10C_3 &= 0{\cdot}585 + 0{\cdot}233\zeta + 0{\cdot}131\eta\zeta - 0{\cdot}118\zeta^2 \\ D_3 &= 0{\cdot}66 - 1{\cdot}414\eta + 0{\cdot}9\eta^2; \end{aligned} \tag{72}$$

(*b*) *for the Lorentz mosaic*:

$$\begin{aligned} A_1 &= 0{\cdot}227 + 0{\cdot}248\eta - 0{\cdot}54\eta^2 \\ B_1 &= 0{\cdot}784 - 0{\cdot}351\eta \\ C_1 &= 0{\cdot}132 - 0{\cdot}577\eta + 0{\cdot}379\eta^2 \\ 10A_2 &= 0{\cdot}046 + 0{\cdot}527\eta - 0{\cdot}336\eta^2 - 0{\cdot}042\eta\zeta \\ B_2 &= 0{\cdot}616 - 0{\cdot}928\eta - 0{\cdot}166\zeta + 0{\cdot}713\eta^2 \\ &\quad + 0{\cdot}147\eta\zeta + 0{\cdot}023\zeta^2 \\ 10A_3 &= (0{\cdot}114 - 0{\cdot}017\zeta)\eta^2 \\ 10B_3 &= 1{\cdot}253 - 0{\cdot}803\eta - 0{\cdot}06\zeta \\ 10C_3 &= 0{\cdot}668 + 0{\cdot}221\zeta + 0{\cdot}119\eta\zeta - 0{\cdot}117\zeta^2 \\ D_3 &= 0{\cdot}819 - 1{\cdot}629\eta + 0{\cdot}975\eta^2. \end{aligned} \tag{73}$$

The factor R was 0·0054 for the Gauss and 0·0027 for the Lorentz distribution. The empirical formula reproduces (65) with an accuracy better than 1% if $y_0 > 0{\cdot}2$.

For $\zeta = 0$ this empirical formula holds also for ellipsoidal crystals if η is replaced by $\eta_0' = \sin\theta_0'$ and χ by $\chi_e = \ln a_e$. For $\zeta \neq 0$, in spite of its decreased accuracy, this formula still conserves two decimal digits in y_0 if $a_0 \leq 5$.

The present theory (as Zachariasen's and BC) gives the primary extinction too, but this must be used with caution. To find it we must set $\zeta = 0$, $\rho_{i0} = \rho_i$ and $\varphi(\gamma) = \Phi_1(4\pi\gamma/3)$ in (64)–(67), where Φ_1 is given by (*B*15*b*). Since $a_e = 1$, y_0 will be just y_{00}, depending on $\eta' = \sin\theta'$ and x_p:

$$x_p = (9/4)Q\rho_1\rho_2 \sin 2\theta/\lambda. \tag{74}$$

An excellent least-squares fit gives the formula (71) where one must take $D_1 = 1{\cdot}25714$ (as above, D_1 is chosen to have the identity at $x = 0$ between the first derivative of the exact and approximate y_0). As a result,

$$\begin{aligned} A_1 &= 0{\cdot}509 + 0{\cdot}255\eta' - 0{\cdot}718\eta'^2 \\ B_1 &= 0{\cdot}139 + 0{\cdot}436\eta' - 0{\cdot}166\eta'^2 \\ C_1 &= -0{\cdot}512 - 0{\cdot}53\eta'^2. \end{aligned} \tag{75}$$

The correction (54) must also be accounted for, with $(\delta_1\delta_2)_p = \sin^2 2\theta'$.

6. Comparison with the Becker & Coppens theory

As we have proved above, differences between the present and the BC theory appear only if the crystal is not of type I. There are two distinct situations: either the average mosaic block can or cannot be approximated by a sphere. In the first case only the second decimal digit in the extinction factor is changed, but significant qualitative and quantitative differences exist in the presence of the anisotropic block shape. In the latter case our extinction factor remains invariant to the permutation of the incident and diffracted directions, a property lost in the BC theory. This can readily be seen from (52). There the general term of the sum is proportional to $\alpha_1^n t^{(n)}$ which after inversion of the particle directions becomes $\alpha_2^n t^{(n)}/a^n \equiv \alpha_1^n t^{(n)}$ [where we have used $\binom{n}{m} = \binom{n}{n-m}$ and $v_{nm} = v_{n,n-m}$]. In the BC theory a is always unity and the last identity in general does not hold. Then the extinction factor is physically incorrect in BC theory if the crystal is of general type with an anisotropic block shape. This would have been of only academic importance if the quantitative differences were small. Fig. 4 speaks for itself. There $1/y_0$ for a spherical crystal with $\mu = 0$, $\theta = 45°$ and Lorentz mosaic distribution is shown *versus* the parameter x from the BC theory. For this particular case the latter is related to the actual x by $x(\text{actual}) = x(\text{BC})(1 + a)/2$. The curve for $a = 1$ is just the BC result. It is seen that even for moderate $a \neq 1$ the relative differences reach 40–50%. For the Gaussian distribution the differences are even greater.

Therefore we can conclude that the results obtained in this paper are of practical importance and may explain some failure in the description of type II or mixed-type secondary extinction.

I am indebted to Dr A. M. Balagurov for encouragement and helpful discussions.

APPENDIX *A*

Becker–Coppens approximation

Here we want to clarify what the approximation used by Becker & Coppens (1974*a*) consists of. This is necessary because there is an error in their paper: the second unlabelled formula on p. 142, as well as the subsequent arguments, are wrong. To arrive at the correct formula [their equation (*B*3)], the oblique hatched area $S(x_1, x_2)$ in Fig. 5(*a*) (partly reproducing Fig. 12 of BC) must be replaced by the horizontally hatched area $S_a(x_1, x_2)$. As a consequence, there are four (not two) regions (Fig. 5*c*) where the approximation acts differently: if (x_1, x_2) is in the region *A*, then $S = S_a$ and there is no approximation; in region *B*, $S < S_a$; $S > S_a$ in *C*; in *D* all three possibilities exist. Hence there are some compensation effects. On the other hand, it is not *a priori* evident that *y* is always overestimated.

Let us use this approximation for our cases. In the first case we must reduce the integral

$$J_1(x_1, x_2) = \int_{S(x_1,x_2)} \mathrm{d}u_1\,\mathrm{d}u_2\,(x_1-u_1)^k(x_2-u_2)^l \times \int_{S(u_1,u_2)} \mathrm{d}v_1\,\mathrm{d}v_2\,(u_1-v_1)^m(u_2-v_2)^n \times t_1^i(v_1, v_2)g(v_2). \qquad (A1)$$

Replacing $S(u_1, u_2)$ by $S_a(u_1, u_2)$ (Fig. 5*b*) we can write

$$J_1(x_1, x_2) = \int_{x_1^0}^{x_1} \mathrm{d}u_1 \int_{u_2^0}^{x_2} \mathrm{d}u_2 (x_1-u_1)^k(x_2-u_2)^l \times \int_{u_2^0}^{u_2} \mathrm{d}v_2\, g(v_2)(u_2-v_2)^n \times \int_{v_1^0}^{u_1} \mathrm{d}v_1 (u_1-v_1)^m(v_1-v_1^0)^i. \qquad (A2)$$

Performing the integral over v_1 and inverting the integrals over u_2 and v_2 one has

$$J_1(x_1, x_2) = \frac{i!m!}{(i+m+1)!} \int_{x_1^0}^{x_1} \mathrm{d}u_1\,(x_1-u_1)^k \times \int_{u_2^0}^{x_2} \mathrm{d}v_2\, g(v_2)(u_1-v_1^0)^{i+m+1} \times \int_{v_2}^{x_2} \mathrm{d}u_2 (x_2-u_2)^l(u_2-v_2)^n. \qquad (A3)$$

Now the integral over u_2 is performed and after that by changing u_2 for v_2 (as an integration variable) one

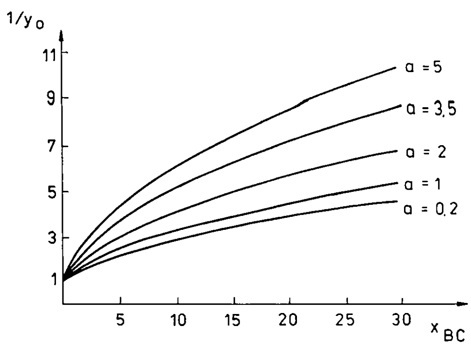

Fig. 4. The inverse of y_0 *versus* x(BC) for different values of the parameter *a*. The crystal is of spherical shape, $\theta = 45°$, $\mu = 0$, Lorentz mosaic distribution.

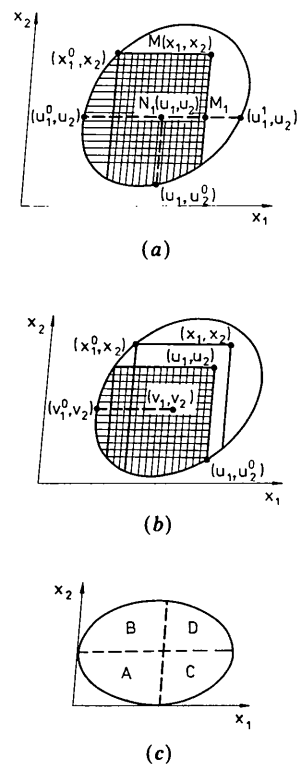

Fig. 5. The BC approximation: the oblique hatched area is replaced by the horizontally hatched area (*a*) in the original paper of BC (1974*a*) and in the present paper for the integral (*A*5), (*b*) in this paper for the integral (*A*1); (*c*) the regions where the BC approximation acts differently.

obtains

$$J_1(x_1,x_2)=\frac{l!\,m!\,n!\,i!}{(l+n+1)!\,(i+m+1)!}\times\int_{S(x_1,x_2)} du_1\,du_2\,g(u_2)\times(x_1-u_1)^k(x_2-u_2)^{l+n+1}t_1^{i+m+1}(u_1,u_2). \quad (A4)$$

In the second case we have to reduce the integral

$$J_2=\int_{S_0} dx_1\,dx_2 f(x_1)t_2^n(x_1,x_2)\times\int_{S(x_1,x_2)} du_1\,du_2\,g(u_2)\times t_1^k(u_1,u_2)(x_1-u_1)^m(x_2-u_2)^l. \quad (A5)$$

Replacing $S(x_1,x_2)$ by $S_a(x_1,x_2)$ (Fig. 5*a*) and following exactly the same path as for J_1 one obtains

$$J_2=\frac{k!\,m!\,n!\,l!}{(m+k+1)!\,(n+l+1)!}\int_{S_0} dx_1\,dx_2 f(x_1)g(x_2)\times t_1^{m+k+1}(x_1,x_2)t_2^{n+l+1}(x_1,x_2). \quad (A6)$$

APPENDIX *B*

Kinematical cross sections for the perfect block of ellipsoidal shape

Let r_i be the principal axes of the ellipsoid oriented along the unit vectors $\mathbf{c}_i$ ($i=1,2,3$). If the ellipsoid is transformed into a sphere of unit radius (see Appendix *C*) and one denotes $\boldsymbol{\beta}=\sum_i r_ih_i\mathbf{c}_i$, then the integral in (2) can be easily performed and for the most probable block one has

$$\sigma(\Gamma_1,\Gamma_2,\Gamma_3)=(4\pi/3)r_1r_2r_3n^2|F|^2\Phi_3(\beta), \quad (B1a)$$

$$\Phi_3(\beta)=9(\sin\beta-\beta\cos\beta)^2/\beta^6. \quad (B1b)$$

If one takes account of (4), (38) and of the transformation (Fig. 1)

$$\boldsymbol{\tau}_i=(1-\delta_{i3})[(-1)^{i-1}\sin\theta\mathbf{n}_1+\cos\theta\mathbf{n}_2]+\delta_{i3}\mathbf{n}_3 \quad (i=1,2,3), \quad (B2)$$

the modulus of β may be expressed as

$$\beta=k_0(\Gamma^{*\prime}\mathsf{A}\Gamma^*)^{1/2} \quad (B3)$$

where

$$\Gamma^{*\prime}=(-\Gamma_1,\Gamma_2,\Gamma_3),\quad \mathsf{A}=\mathsf{BPB}', \quad (B4a,b)$$

$$\mathsf{P}=\mathsf{E}^{(c)\prime}\mathsf{R}^2\mathsf{E}^{(c)},\quad \mathsf{R}_{ij}=r_i\delta_{ij}, \quad (B5a,b)$$

δ_{ij} being the Kronecker symbol and B the matrix of the transformation (*B*2). Now (*B*1) is integrated over Γ_3 to obtain $\sigma(\Gamma_1,\Gamma_2)$. Although difficult, this integral can be performed exactly, but unfortunately the result cannot be convoluted analytically with $W(\varepsilon_3)$. In this situation it is better to approximate $\Phi_3(\beta)$ in the beginning and then integrate over Γ_3. If $W(\varepsilon_3)$ is Gaussian, it is convenient to take

$$\Phi_3(\beta)\simeq\exp(-c_0^2\beta^2/4\pi), \quad (B6)$$

where $c_0=1{\cdot}612\simeq5/3$ is determined from the normalization condition for $\sigma(\Gamma_1,\Gamma_2,\Gamma_3)$. Now, integrating over Γ_3 one has as a result a Gaussian with argument proportional to

$$\omega=\left[\sum_{i,j=1}^{2}(A_{ij}A_{33}-A_{i3}A_{j3})\Gamma_i^*\Gamma_j^*/A_{33}\right]^{1/2}. \quad (B7)$$

By taking into account (*B*4*b*) one has

$$A_{ij}A_{33}-A_{i3}A_{j3}=|\mathsf{P}|[\cos^2\theta P_{11}^{-1}+(-1)^{1+\delta_{ij}}\sin^2\theta P_{22}^{-1}+(-1)^i\delta_{ij}\sin 2\theta P_{12}^{-1}]. \quad (B8)$$

The inverse of P is trivially calculated from (*B*5*a*); replacing it in (*B*8) and comparing with (40) and (41) we can write

$$A_{ij}A_{33}-A_{i3}A_{j3}=|\mathsf{P}|\cos[(1-\delta_{ij})2\theta']/(\rho_1\rho_2). \quad (B9)$$

On the other hand,

$$A_{33}=P_{33}=|\mathsf{P}|[P_{11}^{-1}P_{22}^{-1}-(P_{12}^{-1})^2]=|\mathsf{P}|\sin^2 2\theta'/(\rho_1\rho_2\sin 2\theta)^2 \quad (B10)$$

if (*B*8) and (*B*9) are considered. Finally, we find

$$\omega=(\rho_2^2\Gamma_1^2+\rho_1^2\Gamma_2^2-2\cos 2\theta'\rho_1\rho_2\Gamma_1\Gamma_2)^{1/2}\times\sin 2\theta/\sin 2\theta' \quad (B11)$$

$$\sigma(\Gamma_1,\Gamma_2)=\frac{4\pi}{3c_0}\frac{\sin 2\theta}{\sin 2\theta'}n^2|F|^2\lambda\rho_1\rho_2\times\exp(-\pi c_0^2\omega^2/\lambda^2). \quad (B12)$$

The exact expression is (Popa, unpublished work)

$$\sigma(\Gamma_1,\Gamma_2)=(4\pi\sin 2\theta/5\sin 2\theta')n^2|F|^2\lambda\times\rho_1\rho_2\Phi_2(2\pi\omega/\lambda) \quad (B13a)$$

$$\Phi_2(x)=15\sum_{k=0}^{\infty}(-1)^kx^{2k}\times[(2k+3)(2k+5)k!(k+1)!]^{-1}. \quad (B13b)$$

Integrating (*B*12) over Γ_2, one gets

$$\sigma(\Gamma_1)=Q(c_0/\lambda)\rho_2\sin 2\theta\times\exp[-\pi(c_0^2/\lambda^2)\rho_2^2\sin^2 2\theta\Gamma_1^2], \quad (B14)$$

the exact expression being (BC)

$$\sigma(\Gamma_1)=Q(3/2\lambda)\rho_2\sin 2\theta\,\Phi_1[(2\pi/\lambda)\rho_2\sin 2\theta\Gamma_1] \quad (B15a)$$

$$\Phi_1(x)=(x^2-x\sin 2x+\sin^2 x)/x^4. \quad (B15b)$$

The Lorentzian approximation of ($B15b$) needed in § 4 is

$$\Phi_1(x) \simeq (1+9x^2/16)^{-1}. \qquad (B16)$$

For $\sigma_2(\Gamma_2)$ the same expressions are obtained with ρ_1 in place of ρ_2.

APPENDIX C
Transformation of the ellipsoid into a sphere of unit radius

Remember here some mathematical relations used above (see also Becker & Coppens, 1975). If the equation of an ellipsoidal surface in the system ($\mathbf{c}_i$) of its principal axes is $\sum_i z_i^2/r_i^2 = 1$ and the transformation $z_i = r_i z_i'$ is performed then this equation become $\sum_i z_i'^2 = 1$, which represents a sphere of unit radius. By this transformation any unit vector $\mathbf{u} = \sum_i u_i \mathbf{c}_i$ is transformed into the vector $\mathbf{U}' = \sum_i U_i' \mathbf{c}_i = \sum_i u_i \mathbf{c}_i / r_i$. If one denotes by ρ_u the ellipsoid radius along the vector $\mathbf{u}$, then the vector $\rho_u \mathbf{u}$ is transformed into $\mathbf{u}' = \rho_u \mathbf{U}'$ of unit length. In consequence we can write

$$1/\rho_u^2 = \sum_i u_i^2/r_i^2. \qquad (C1)$$

Now, if $\mathbf{u}$ and $\mathbf{v}$ are a pair of unit vectors whose mutual angle is φ, after transformation this angle becomes

$$\cos \varphi' = \mathbf{u}' . \mathbf{v}' = \rho_u \rho_v \sum_i u_i v_i / r_i^2. \qquad (C2)$$

Finally, if t is a segment in the $\mathbf{u}$ direction, the vector $t\mathbf{u}$ is transformed into $t\mathbf{U}' = t|\mathbf{U}'|\mathbf{u}' = t'\mathbf{u}'$. Then the transformation t' of t is

$$t' = t/\rho_u. \qquad (C3)$$

References

BECKER, P. J. (1977). *Acta Cryst.* **A33**, 243-294.
BECKER, P. J. & COPPENS, P. (1974*a*). *Acta Cryst.* **A30**, 129-147.
BECKER, P. J. & COPPENS, P. (1974*b*). *Acta Cryst.* **A30**, 148-153.
BECKER, P. J. & COPPENS, P. (1975). *Acta Cryst.* **A31**, 417-425.
COPPENS, P. & HAMILTON, W. C. (1970). *Acta Cryst.* **A26**, 71-83.
DARWIN, C. G. (1922). *Philos. Mag.* **43**, 800-824.
HAMILTON, W. C. (1957). *Acta Cryst.* **10**, 629-634.
HARADA, J., MIYATAKE, H. & SAKATA, M. (1984). *Acta Cryst.* **A40**, C357.
HUTTON, J., NELMES, R. J. & SCHEEL, H. J. (1981). *Acta Cryst.* **A37**, 916-920.
KATO, N. (1976*a*). *Acta Cryst.* **A32**, 453-457.
KATO, N. (1976*b*). *Acta Cryst.* **A32**, 458-466.
KATO, N. (1979). *Acta Cryst.* **A35**, 9-16.
KATO, N. (1980). *Acta Cryst.* **A36**, 763-769.
KAWAMURA, T. & KATO, N. (1983). *Acta Cryst.* **A39**, 305-310.
NELMES, R. J. (1980). *Acta Cryst.* **A36**, 641-653.
POPA, N. C. (1976). *Acta Cryst.* **A32**, 635-641.
SEARS, V. F. (1975). *Adv. Phys.* **24**, 1-45.
SEARS, V. F. (1978). *Can. J. Phys.* **56**, 1261-1288.
SUORTTI, P. (1982). *Acta Cryst.* **A38**, 642-647.
TOMIYOSHI, S., YAMADA, M. & WATANABE, H. (1980). *Acta Cryst.* **A36**, 600-604.
VINEYARD, G. H. (1954). *Phys. Rev.* **96**, 93-98.
WERNER, S. A. (1974). *J. Appl. Phys.* **45**, 3246-3254.
ZACHARIASEN, W. H. (1967). *Acta Cryst.* **23**, 558-564.

Acta Cryst. (1987). **A43**, 316-321

X-ray Diffraction by a Low-Angle Twist Boundary Perpendicular to Crystal Surface. I. Superstructure Factor of Screw Dislocation Superlattice

BY D. M. VARDANYAN

Department of Physics, Yerevan State University, Mravyan str. 1, 375049 *Yerevan, Armenia, USSR*

AND H. M. PETROSYAN

Department of Physics, Yerevan Pedagogical Institute, Khandjyan str. 5, 375010 *Yerevan, Armenia, USSR*

(*Received* 12 *August* 1985; *accepted* 21 *October* 1986)

Abstract

The X-ray two-wave diffraction on a dislocation wall perpendicular to a crystal surface, consisting of periodically arranged dislocations (low-angle twist boundary), is considered in the case when the dislocation superlattice period is much less than the crystal extinction length. The formula obtained for the reflected intensity is of the same form as that for an ideal crystal with a modified crystal structure factor. The superstructure factor of a dislocation superlattice is calculated. The recurrence relations are produced which enable a superstructure factor to be calculated for a satellite of any order and magnitude **hb** (**h** is the diffraction vector, **b** is the Burgers vector).

1. Introduction

The grain boundary (GB) is a surface between two misorientated single crystals. The dislocation structure of a GB is well known (Hirth & Lothe, 1968;

0108-7673/87/030316-06$01.50